Catalysis Today 149 (2010) 413–417

Contents lists available at ScienceDirect

Catalysis Today

journal homepage: www.elsevier.com/locate/cattod

Catalytic activity evaluation for hydrogen production via autothermal reforming of methane

Aleksándros El Áurens Meira de Souza *, Leonardo José Lins Maciel, Nelson Medeiros de Lima Filho, Cesar Augusto Moraes de Abreu

LPC/DEQ/CTG, Universidade Federal de Pernambuco, Av. Prof. Artur de Sá, s/n°, Cidade Universitária, Recife-PE 50.740-521, Brazil

ARTICLE INFO

Article history:
Available online 31 August 2009

Keywords:
Autothermal reforming
Methane
Nickel
Gamma-alumina
Hydrogen

ABSTRACT

A nickel catalyst (5.75 wt.%) supported on gamma-alumina was evaluated through autothermal reforming of methane (ATR). The reforming process was pointed to hydrogen production, following thermodynamic and stoichiometric predictions. The catalyst was characterised by several methods including atomic absorption spectroscopy (AAS), B.E.T.-N_2, X-ray diffraction (XRD), scanning electron microscope (SEM) and thermal analyses (thermogravimetry, TG; derivate thermogravimetry, DTG; and differential thermal analysis, DTA). Experimental evaluations in a fixed-bed reactor (1023–1123 K, 1.00 bar, 150–400 cm^3/min feed) presented methane conversions in the range of 40–65%. The effluent mixtures provided hydrogen yields in the range of 78–84%, carbon monoxide 3–14%, and carbon dioxide 5–18%. High molar H_2/CO ratios, ranging from 8 to 90, were obtained. Operating autothermal conditions (excess of steam, 1023–1123 K, 1.00 bar) provided low coke formation and high hydrogen selectivity (81%) for methane reforming.

1. Introduction

Natural gas (NG) has high contents of methane in its composition (66.0–97.8%, v/v), can be processed in the presence of steam and oxygen via autothermal catalytic reforming.

Autothermal reforming of methane (ATR) is a combination of the conventional steam reforming of methane (SRM) and the non-catalytic partial oxidation of methane (POX or NC-POM) [1,2]. In this process, a mixture of natural gas, oxygen and water is firstly submitted to a non-catalytic partial oxidation, and then the products are converted into syngas through reforming reactions. Syngas from NG, a mixture of carbon monoxide and hydrogen, may be used to produce high added value chemicals such as hydrocarbons, fuels [1], and oxygenated compounds [2]. In gas-to-liquids (GTL) processes, where natural gas is firstly converted to syngas, 60–70% of the costs of the overall process are associated with the syngas production.

The main obstacle of the reforming processes is the catalyst deactivation due to carbon deposition during the reaction. The catalytic partial oxidation and steam introduction may drastically decrease or even eliminate the carbon deposition [1,3].

Nickel catalysts, traditionally used in industrial steam reforming processes of NG, have presented good performances in terms of conversion and selectivity to obtain syngas by methane reforming, although these systems are sensible to coke formation.

In this work, in order to have a stable syngas and/or hydrogen production and minimum activity losses, a nickel/gamma-alumina supported catalyst was prepared and employed in the ATR process. Based on stoichiometric predictions, a thermodynamic analysis [4–14] was performed, establishing the operational conditions of the evaluation process.

2. Experimental

The catalyst was prepared employing nickel nitrate ($Ni(NO_3)_2{\cdot}6H_2O$, Sigma) and gamma-alumina (γ-Al_2O_3, Degussa) as a catalytic support. The preparation method was the incipient wetness where alumina was impregnated with the nickel nitrate solution. Firstly, the impregnated solution was evaporated to dryness. Then, the solid was dried at 393 K for 12 h, and calcinated at 873 K in air flow during 5 h. Finally, to promote the activation, the material was reduced in hydrogen atmosphere at 1073 K for 2 h.

The nickel catalyst was characterised by atomic absorption spectroscopy (AAS, Varian AA 220 FS), B.E.T.-N_2 (Micromeritcs ASAP 2010), X-ray diffraction (XRD, Siemens D5000), scanning electron microscope (SEM, Jeol JSM-6360), thermal analyses (TG, DTG and DTA, Shimadzu TGA-50) and elementary carbon analysis.

The autothermal reforming experiments were carried out in a fixed-bed reactor packed with nickel catalyst (d_p = 212 μm, m = 60 mg) under atmospheric pressure, and at three different temperatures 1023, 1073, and 1123 K, respectively [10]. The reactants were fed into the reactor with a gas mixture with a molar ratio of CH_4:O_2:H_2O = 5:1:9, diluted in argon at 56% (v/v) with a flow rate in

* Corresponding author. Tel.: +55 81 2126 7289.
E-mail address: aleksandros@ig.com.br (de Souza).

0920-5861/$ – see front matter © 2009 Elsevier B.V. All rights reserved.
doi:10.1016/j.cattod.2009.06.003

the range of 150–400 cm^3/min (STP). The reactor effluents, residual reagents and products were analysed on-line by gas chromatograph (GC, Saturn 2000, Varian; TCD, Carbosphere/Porapak-Q).

3. Results and discussion

3.1. Feed composition

Prior to operations, the stoichiometric relations, predicting the operating conditions where carbon deposition on the catalyst was avoided, were established. So, the autothermal reforming reaction equation was written as

$$CH_4 + aO_2 + bH_2O \rightarrow cCO + dCO_2 + eH_2 \quad (1)$$

The stoichiometric adjustment lead to the following relations: $b = e - 2$, $c = 2 - 2a - b$ and $d = 2a + b - 1$. To maximise the H_2 production ($c = 0$), $d = 1$ and $a = 1 - b/2$. For $a \geq 0 \rightarrow b \leq 2$, a straight line describes the feed composition possibilities to the ATR (Fig. 1).

In Fig. 1, detached lines show positions with stoichiometric relations (H_2O/CH_4 vs. O_2/CH_4) where carbon deposition should be avoided [3]. Thus, to avoid coke deposition, the feed was carried out at CH_4:O_2:H_2O = 5:1:9 molar ratios, in the avoidable coking region of the SRM.

Based on the molar ratio of the feed, a condition was obtained (Eq. (2)), adopting a stoichiometric steam excess as indicated [15]:

$$CH_4 + 0.2O_2 + 1.8H_2O \rightarrow CO_2 + 3.6H_2 + 0.2H_2O \quad (2)$$
$$\Delta H = +109\ kJ/mol$$

This condition overcame the athermicity of the reaction [12–14] (exothermicity), producing a sufficient quantity of energy to reach the autothermicity.

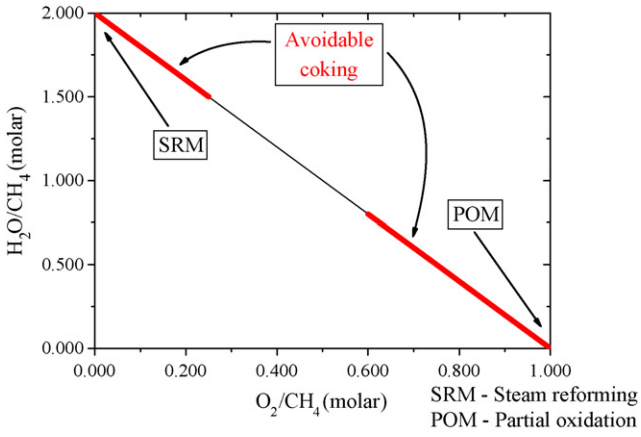

Fig. 1. Stoichiometric relations for autothermal reforming of methane to maximise the hydrogen production.

Table 1
B.E.T. analysis of pre-catalytic material and catalyst.

Material	B.E.T. area (m^2/g)	Pore diameter (Å)	Pore volume (cm^3/g)	Micropore volume (cm^3/g)
Alumina *in natura*	226	68	0.4	n.d.
Pre-treated alumina	145	102	0.4	0.0006
Calcinated catalyst	105	125	0.3	0.0026
Reduced catalyst	107	129	0.3	0.0034

n.d.: not determinated.

3.2. Catalytic characterisations

The nickel content and its surface area, characterised by AAS and B.E.T.-N_2, were 5.75% by weight and 1067 m^2/g, respectively. Through textural analyses (Table 1), reductions of specific surface area and pore volume during the catalyst preparation up to the calcination step were observed. This can be explained by the metal deposition on the support. During the reduction step, the pore volume increases, indicating NiO conversion into nickel.

X-ray diffratograms of the catalyst preparation steps allowed to identify the solid phases. From the crystallographic patterns of alumina, it was possible to identify a gamma-alumina phase on the support *in natura* and on the support submitted to the thermal pre-treatment. There was no evidence of gamma-alumina transition to delta-alumina. XRD analysis of the catalyst, performed after the calcinations step, identified nickel oxide presence, as well as nickel aluminates $NiAl_2O_4$ ($2\theta = 37.0^\circ$ and 59.7°) [16] and $NiAl_{10}O_{16}$ ($2\theta = 19.1^\circ$, 45.5° and 66.8°). After reduction step, the analysis also identified the presence of the reduced nickel ($2\theta = 44.5^\circ$ and 51.8°).

Scanning electron microscope (SEM) analyses of the catalyst samples were performed before and after the reforming operations, when coke as whiskers forms [11,17] on the catalyst was identified (Fig. 2).

Fig. 3 presents thermal analyses (TG, DTG and DTA) of the catalyst during the preparation steps. The TG plot exhibited the initial calcinations temperature of the precursor. The DTG profile presented a peak at 346.9 K indicating a loss of water of 13.0% between 298.7 and 427.9 K. A second peak was observed at 537.3 K indicating a loss of NO_2 of 10.0%, between 427.9 and 814.5 K. There is also an indication that both events overlap in the range of 298.7 until 814.5 K. Losses progressed to 1273 K possibly due to NO_x emissions.

The carbon deposited during the reaction process was obtained from thermal analyses (TG and DTG, Fig. 4) of the catalyst. It showed a carbon mass loss of 4.2% between 430.7 and 1081.5 K. Higher carbon deposit levels on the catalyst (>70% in weight) were found under drastic operating conditions [18,19]. A mass loss of water of 7.2% occurred in the range 300.1–430.7 K (endothermic peak).

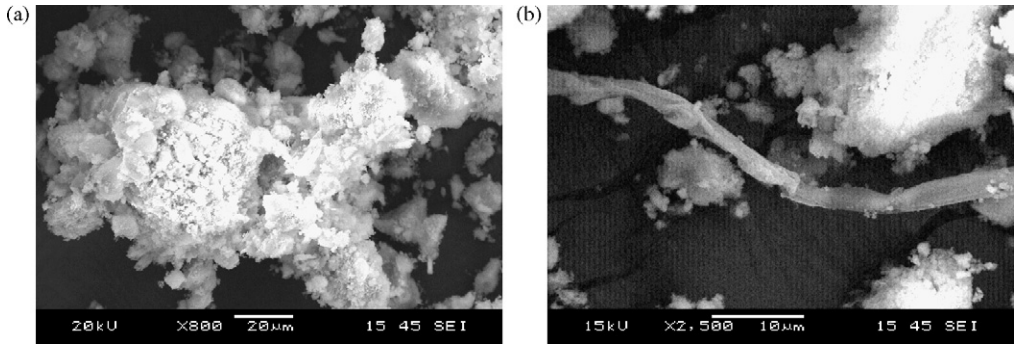

Fig. 2. Electronic micrographies of Ni(5.75 wt.%)/γ-Al_2O_3 catalyst. (a) Before autothermal reforming (400×) and (b) after autothermal reforming (2500×).

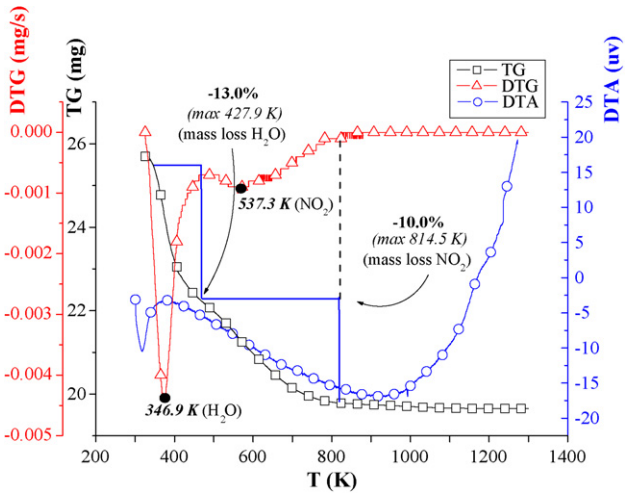

Fig. 3. Thermal analysis of the catalyst during the preparation steps.

3.3. Catalytic evaluations

Experimental evaluations of the ATR process, performed in a fixed-bed continuous reactor, as a function of the operational time, showed that steady states of concentration were reached after 100 min of operation. Under the same pressure conditions (1.00 bar) and feed composition (molar ratio CH_4:O_2:H_2O = 5:1:9). For each temperature, flow rates in the range of 150–400 cm^3/min in the presence of the nickel catalyst (60 mg, Ni(5.75 wt.%)/γ-Al_2O_3) were employed. As a function of the utilised flow rates, the process was operated with different spatial times (9–24 kg s/m^3, or $GHSV = 331.5 \times 10^3$–884.0×10^3 h^{-1}). The spatial times (τ) is defined as the ratio of the mass of the catalyst to the volumetric flow of reactants at standard conditions (298 K and 1.00 bar):

$$\tau = \left(\frac{m_{cat}}{\dot{Q}_{inlet}}\right)_{STP} \quad (3)$$

where m_{cat} is the mass of the catalyst, kg, and $\dot{Q}_{inlet}$ is the volumetric flow rate of the reactants, m^3/h.

The gas hours space velocity (*GHSV*) is defined as the ratio of the volumetric flow of reactants at standard conditions (298 K and 1.00 bar) to the total catalyst volume and has units of inverse time, or:

$$GHSV = \left(\frac{\rho_{cat}\dot{Q}_{inlet}}{m_{cat}}\right)_{STP} \quad (4)$$

where ρ_{cat} is the density of the catalyst, kg/m^3, and $\dot{Q}_{inlet}$ and m_{cat} were already defined.

Catalytic activity (A) was obtained in terms of methane consumption:

$$A = \frac{-r_{obs}}{-r^o} \quad (5)$$

where $-r_{obs}$ and $-r^o$ are the instantaneous and initial reaction rates, mol g_{cat}^{-1} h^{-1}.

In Fig. 5, the evolutions of the catalytic activity are presented as a function of the spatial time for the three operating temperatures. It was observed that, for operations with higher spatial times, the catalytic activity was the lowest (Fig. 5). Evolutions showed that the activities decreased approximately 8%, at each temperature. From 1023 to 1123 K, for all spatial times, a reduction of the catalytic activity, circa of 23%, was observed. This occurred possibly due to the deposition of carbon in methane cracking step, at higher temperatures (endothermic process), mainly at initial conditions ($-r^o$), with additional production of carbon.

The experimental steady state values of the concentrations indicated CH_4 conversions and production of CO_2, CO, H_2 and carbon. Based on these experimental data and on the set of reaction mechanisms of the ATR and other reforming processes proposed by several authors [3,20–29], the following major reaction steps were proposed: heterogeneous methane catalytic cracking, homogeneous methane combustion, water–gas shift reaction, and heterogeneous non-catalytic carbon consumption with carbon dioxide (Boudouard reverse reaction).

Hydrogen and carbon monoxide productions allowed calculating the syngas yields (Y_{syngas}) and H_2/CO molar ratio.

$$Y_{syngas} = \frac{Y_{H_2} + Y_{CO}}{2} \quad (6)$$

where $Y_{H_2} = C_{H_2}/C_{H_2,max}$, $Y_{CO} = C_{CO}/C_{CO,max}$, C_i is the obtained concentration, mol/m^3, of the specie i, and $C_{i,max}$ = mol/m^3 obtained to maximum reagents conversion.

For the three operating temperatures, the plots (Fig. 6) are represented as spatial time functions and they indicate that the syngas yields increases while H_2/CO molar ratios decrease. The syngas yields were in the range from 10 to 61% and the highest

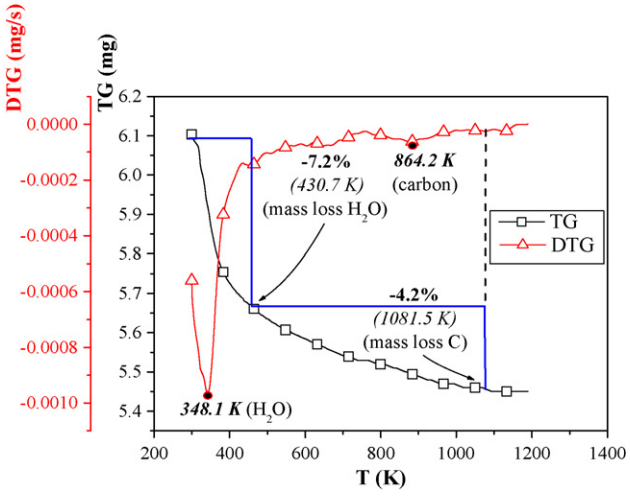

Fig. 4. Thermogravimetric (TG) and derivate thermogravimetric (DTG) analysis of the nickel catalyst. Determination of mass loss of deposited carbon in autothermal reforming of methane. Operating conditions: 1123 K, 1.00 bar, total feed flow rate 400 cm^3/min, feed molar ratio CH_4:O_2:H_2O = 5:1:9, Ni(5.75 wt.%)/γ-Al_2O_3.

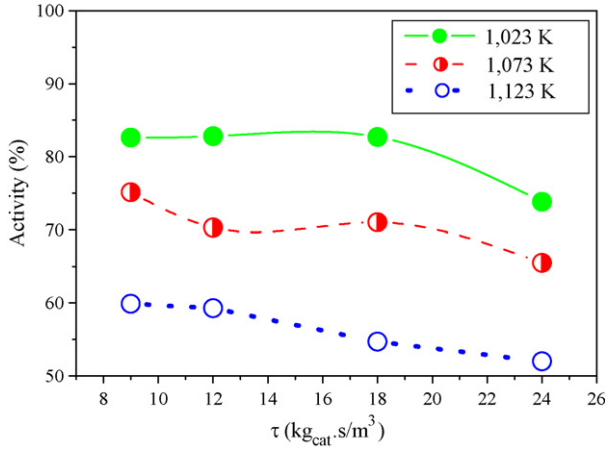

Fig. 5. Evolution of the catalytic activity in the autothermal reforming of methane. Temperature effect. Operating conditions: feed molar ratio CH_4:O_2:H_2O = 5:1:9; 1.00 bar; Ni(5.75 wt.%)/γ-Al_2O_3; 2 h of operation.

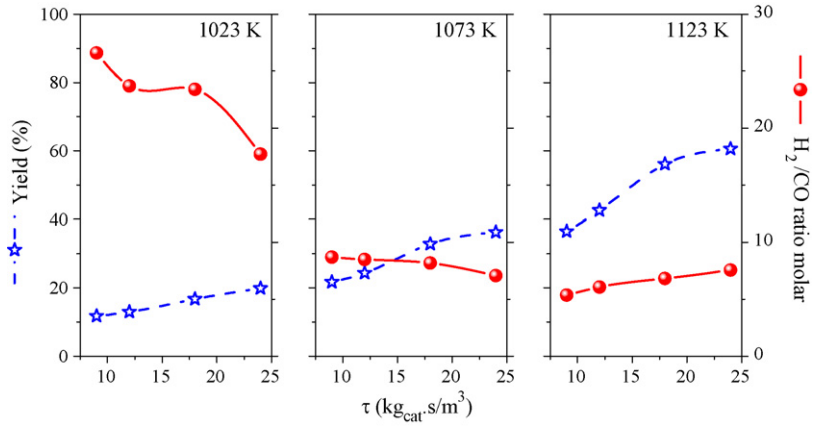

Fig. 6. Evolutions of the syngas yield and H_2/CO molar ration in the autothermal reforming of methane. Temperature effect. Operating conditions: feed molar ratio CH_4:O_2:H_2O = 5:1:9; 1.00 bar; Ni(5.75 wt.%)/γ-Al_2O_3; 2 h of operation.

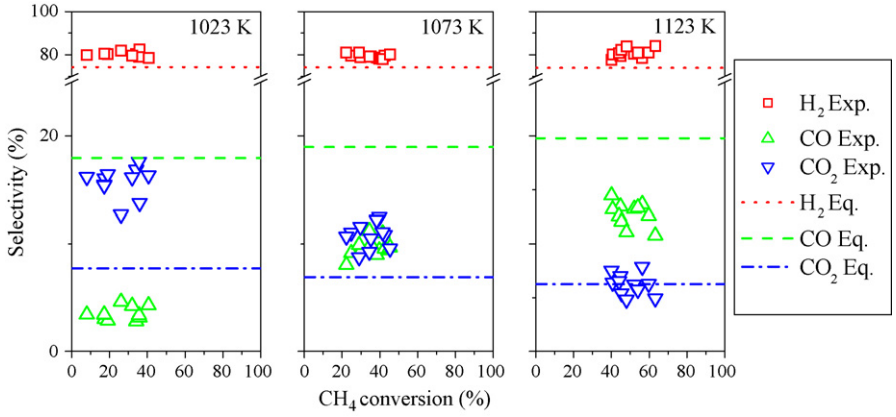

Fig. 7. Selectivities of the products in function of methane conversion in the autothermal reforming of methane. Operating conditions: feed molar ratio CH_4:O_2:H_2O = 5:1:9; 1.00 bar; Ni(5.75 wt.%)/γ-Al_2O_3; 2 h of operation. (Exp.: experimental; Eq.: thermodynamic equilibrium).

yield was obtained at 1123 K. The H_2/CO molar ratio decreased with the temperature, from 27 to 8, with the highest hydrogen production at 1023 K.

The selectivity levels (S_i) as a function of the analysed species H_2, CO and CO_2, at different spatial times are presented in Fig. 7.

$$S_i = 10^2 \frac{C_i}{\Sigma C_p} \quad (7)$$

where C_i is the obtained concentration, mol/m^3, of the specie *i*, and C_p is the obtained concentration, mol/m^3, of all the products.

From the autothermal reaction (Eq. (2)), equilibrium selectivities were calculated (dotted lines), via van't Hoff's, and compared with experimental results.

The experimental results indicated that the process was selective to hydrogen production and in a range from 78 to 84%, according thermodynamic predictions. Carbon dioxide and carbon monoxide had maximum selectivities of 18 and 14%, respectively. An approximate constant level of hydrogen selectivity, with a decreasing H_2/CO molar ratio, indicated the occurrence of consumption of carbon by carbon dioxide into carbon monoxide (Boudouard reverse reaction).

4. Conclusions

A kinetic-operational procedure was applied to the evaluation of the autothermal reforming of methane. A supported nickel catalytic, Ni(5.75 wt.%)/γ-Al_2O_3, was formulated, and experimental tests of its activity, as well as operational evaluations of the process, were performed. Predominant presence of the nickel phase and nickel oxide and nickel aluminates phases (NiO, $NiAl_2O_4$, $NiAl_{10}O_{16}$) were detected in the catalyst. Coke formation as whisker forms was identified.

Stoichiometric predictions and thermodynamic analysis indicated operational autothermal conditions (excess of steam, 1023–1123 K, 1.00 bar) providing low coke formation (4.2 wt.%).

At 1123 K, the highest syngas yield, 61%, and the lower H_2/CO molar ratio were obtained. A high hydrogen selectivity (81%) was quantified at the three operating temperature.

Acknowledgements

We would like to acknowledge PPEQ/UFPE, FINEP and PETROBRAS, for the financial support to this project.

References

[1] M.A. Peña, J.P. Gómez, J.L.G. Fierro, Appl. Catal. A 144 (1996) 7–57.
[2] H.A/S Topsøe, Societé Belge de L'Azote, Hydrocarbon Process. Int. Ed. 67 (4) (1988), 77.
[3] S.H. Chan, H.M. Wang, Int. J. Hydrogen Energy 25 (5) (2000) 441–449.
[4] J.H. Edwards, A.M. Maitra, Fuel Process. Technol. 42 (1995) 269–289.
[5] M.G. Poirier, C. Sapundzhiev, Int. J. Hydrogen Energy 22 (4) (1997) 429–433.
[6] S. Ahmed, M. Krumpelt, Int. J. Hydrogen Energy 26 (2001) 291–301.
[7] A.E. Lutz, R.W. Bradshaw, L. Bromberg, A. Rabinovich, Int. J. Hydrogen Energy 29 (2004) 809–816.
[8] T.A. Semelsberger, L.F. Brown, R.L. Borup, M.A. Inbody, Int. J. Hydrogen Energy 29 (2004) 1047–1064.
[9] Y.-S. Seo, A. Shirley, S.T. Kolaczkowski, J. Power Sources 108 (2002) 213–225.

[10] A. Ersoz, H. Olgun, S. Ozdogan, C. Gungor, F. Akgun, M. Tiris, J. Power Sources 118 (2003) 384–392.
[11] J.A.C. Dias, J.M. Assaf, J. Power Sources 137 (2004) 264–268.
[12] S. Ayabe, H. Omoto, T. Utaka, R. Kikuchi, K. Sasaki, Y. Teraoka, K. Eguchi, Appl. Catal. A 241 (2003) 261–269.
[13] B.F. Hagh, Int. J. Hydrogen Energy 28 (12) (2003) 1369–1377.
[14] S.H.D. Lee, D.V. Applegate, S. Ahmed, S.G. Calderone, T.L. Harvey, Int. J. Hydrogen Energy 30 (8) (2005) 829–842.
[15] K. Takehira, T. Shishido, P. Wang, T. Kosaka, K. Takaki, J. Catal. 221 (2004) 43–54.
[16] S.S. Maluf, E.M. Assaf, J.M. Assaf, Quím. Nova 26 (2) (2003) 181–187.
[17] J.-W. Snoeck, G.F. Froment, M. Fowles, J. Catal. 169 (1997) 250–262.
[18] J.H. Bitter, K. Seshan, J.A. Lercher, J. Catal. 183 (1999) 336–343.
[19] C.A.M. Abreu, D.A. Santos, J.A. Pacífico, N.M. Lima Filho, Ind. Eng. Chem. Res. 47 (2008) 4617–4622.
[20] D.L. Trimm, C.-M. Lam, Chem. Eng. Sci. 35 (1980) 1405–1413.
[21] J. Xu, G.F. Froment, AIChE J. 35 (1989) 88–96.
[22] J. Xu, G.F. Froment, AIChE J. 35 (1989) 97–103.
[23] K. Sheshan, H.M. Barge, W. Hally, A.M.J. van Keullen, J.R.H. Ross, Carbon dioxide reforming of methane in the presence of nickel and platinum catalysts supported on ZrO_2, Stud. Surf. Sci. Catal. 81 (1994) 285–290.
[24] L. Ma, D.L. Trimm, Appl. Catal. A 138 (1996) 265–273.
[25] S. Wang, G.Q. Lu, Role of CeO_2 in Ni/CeO_2–Al_2O_3 catalysts for carbon dioxide reforming of methane, Appl. Catal. B 19 (1998) 267–277.
[26] C. Chen, M. Horio, T. Kojima, Chem. Eng. Sci. 55 (2000) 3861–3874.
[27] W. Jin, X. Gu, S. Li, P. Huang, N. Xu, J. Shi, Chem. Eng. Sci. 55 (2000) 2617–2625.
[28] D.L. Hoang, S.H. Chan, Appl. Catal. A 268 (2004) 207–216.
[29] F. Bustamante, R.M. Erick, A.V. Cugini, R.P. Killmeyer, B.H. Howard, K.S. Rothenberger, M.V. Ciocco, B.D. Morreale, Hightemperatures kinetics of the homogeneous reverse water–gas shift reaction, AIChE J. 50 (5) (2004) 1028–1041.